

THE INTRACLUSTER MEDIUM IN $Z > 1$ GALAXY CLUSTERS

S.A. STANFORD¹, BRADFORD HOLDEN¹

Physics Department, University of California-Davis, Davis, CA 95616, USA

PIERO ROSATI

European Southern Observatory, Karl-Scharzschild-Strasse 2, D-85748 Garching, Germany

PAOLO TOZZI, STEFANO BORGANI

Osservatorio Astronomico di Trieste, via G.B. Tiepolo 11, I-34131, Trieste, Italy

PETER R. EISENHARDT

Jet Propulsion Laboratory, California Institute of Technology, MS 169-327, 4800 Oak Grove, Pasadena, CA 91109

AND

HYRON SPINRAD

Astronomy Department, University of California, Berkeley, CA 94720

Draft version October 30, 2018

ABSTRACT

The Chandra X-ray Observatory was used to obtain a 190 ks image of three high redshift galaxy clusters in one observation. The results of our analysis of these data are reported for the two $z > 1$ clusters in this Lynx field, which are the most distant known X-ray luminous clusters. Spatially-extended X-ray emission was detected from both these clusters, indicating the presence of hot gas in their intracluster media. A fit to the X-ray spectrum of RX J0849+4452, at $z = 1.26$, yields a temperature of $kT = 5.8^{+2.8}_{-1.7}$ keV. Using this temperature and the assumption of an isothermal sphere, the total mass of RX J0849+4452 is found to be $4.0^{+2.4}_{-1.9} \times 10^{14} h_{65}^{-1} M_{\odot}$ within $r = 1 h_{65}^{-1}$ Mpc. The T_x for RX J0849+4452 approximately agrees with the expectation based on its $L_{bol} = 3.3^{+0.9}_{-0.5} \times 10^{44}$ erg s⁻¹ according to the low redshift $L_x - T_x$ relation. The very different distributions of X-ray emitting gas and of the red member galaxies in the two $z > 1$ clusters, in contrast to the similarity of the optical/IR colors of those galaxies, suggests that the early-type galaxies mostly formed before their host clusters.

Subject headings: galaxies: clusters: general; X-rays: general

1. INTRODUCTION

Numerical simulations based on hierarchical clustering models such as cold dark matter (CDM) show the rate at which clusters form depends critically on Ω_m , and weakly on Λ and the initial power spectrum. Thus, the observed evolution of the cluster number density of a given X-ray temperature and luminosity can determine Ω_m . Oukbir & Blanchard 1992, Eke et al. 1998a. A critical component of such a measurement is an understanding of the thermodynamical evolution of the intracluster medium (ICM) Bower 1997, Borgani et al. 1999, Tozzi & Norman 2000.

The study of ICM properties at high z is mostly unexplored territory. Until the advent of Chandra and XMM, X-ray observations with limited resolution and sensitivity were unable to provide conclusive measurements of the ICM at $z > 1$ associated with bona fide galaxy clusters. For example, ROSAT observations of high z radio galaxies possibly associated with galaxy clusters Crawford & Fabian 1996 provided only limited evidence that the observed X-ray emission originates from hot intracluster gas.

To assemble a well-defined sample for studying the properties of the ICM and cluster galaxy populations at $z > 1$, we have been using near-IR imaging and deep optical spectroscopy to complete the identification of the faintest candidate clusters in the Rosat Deep Cluster Sur-

vey (RDCS) Rosati et al. 1995, Rosati et al. 1998. Of the 4 RDCS clusters which have been identified at $z > 1$, two are separated by only 4.2 arcmin on the sky and 0.01 in redshift: RX J0848+4453 at $z = 1.27$ Stanford et al. 1997 and RX J0849+4452 at $z = 1.26$ Rosati et al. 1999. Keck LRIS spectroscopy has confirmed 20 member galaxies in these two clusters. In addition, a third moderate redshift cluster in this Lynx field already had been identified from the RDCS, RX J0848+4456 at $z = 0.56$ (Rosati et al. 1998; the Chandra results on this object will be presented elsewhere: Holden et al., in preparation). The Lynx field offers the opportunity to probe the physical parameters of the ICM over the redshift range 0.6–1.3 in a single deep Chandra pointing. $H_0 = 65$ km s⁻¹ Mpc⁻¹, $\Omega_m = 0.3$, and $\Lambda = 0.7$ are assumed throughout this paper.

2. OBSERVATIONS AND REDUCTIONS

New Lynx field X-ray data were obtained by Chandra using the Advanced CCD Imaging Spectrometer imaging (ACIS-I) detector. Two exposures were obtained in the faint mode when ACIS was at a temperature of -120 K. The first observation (Obs ID 1708) was taken on 2000 May 3 for 65 ks, and the second (Obs ID 927) on 2000 May 4 for 125 ks.

The Level 1 data were processed using the calibration files available as of 15 September 2000 for the aspect so-

¹Institute of Geophysics and Planetary Physics, Lawrence Livermore National Laboratory

lution and the quantum efficiency uniformity, which correct the effective area for loss due to charge transfer inefficiency. The data were filtered to include only the standard event grades 0, 2, 3, 4, and 6. All hot pixels and columns were removed, as were the columns close to the border of each node, since the grade filtering is not efficient in these columns. The removal of columns and pixels slightly reduces the effective area of the detector, the effect of which has been included when calculating the total exposure maps. Time intervals with background rates larger than 3σ over the quiescent value ($0.30 \text{ counts s}^{-1}$ per chip in the 0.3 - 10 keV band) were removed. This procedure gave 61 ks of effective exposure in the first observation, and 124 ks in the second, for a total of 185 ks.

3. RESULTS

Both $z > 1$ clusters were detected and found to contain spatially extended X-ray emission (left panel of Figure 1). The emission in RX J0848+4453 is weak and amorphous, while in RX J0849+4452 it is symmetric and centrally concentrated in a way similar to that seen in relaxed clusters at lower redshift. The radial surface brightness profile for RX J0849+4452 is shown in the right panel of Figure 1 along with a β model fit. In both clusters there are relatively strong point sources within the ROSAT detection area. In both cases, approximately 40% of the flux as measured by ROSAT is from point sources unlikely to be associated with the clusters, showing the importance of obtaining high spatial resolution data. Further analyses of the point sources found in the Chandra observation, including their optical-IR identifications, will be presented by Stern et al. (in preparation).

The spectra of the two clusters were determined in the following way. After removing the point sources, events at 0.5–6.0 keV in an $r = 35''$ (~ 0.32 Mpc) circular aperture centered on each cluster were extracted. Events in a surrounding background region, with the cluster and point sources excised, were also extracted. The background model consists of a broken power law and a Gaussian for the instrumental Au emission line at 2.1 keV. The background models for both clusters were fit separately and agree with each other within the calculated errors. The normalization of these background models was rescaled by the relative areas of the background region and the cluster apertures. The number of net counts in the 0.5–6.0 keV range is 182 and 430 for RX J0848+4453 and RX J0849+4452, respectively, within the $r = 35''$ aperture after the removal of point sources and the background. Figure 2 shows the unfolded spectra (see below), which were divided into bins of 40 events before background subtraction.

To determine the X-ray temperatures and fluxes, Raymond-Smith (1977) model spectra with absorption were folded through the appropriate response matrices and fit to the data, while the background model was held fixed, using a maximum-likelihood test with the statistic from Cash (1979). The column density was fixed at $n(H) = 2.0 \times 10^{20} \text{ cm}^{-2}$, which agrees fairly well with both the $n(H)$ obtained from the $100\mu\text{m}$ maps of Schlegel et al. (1998), and that derived using Dickey & Lockman (1990). The metallicity of the model spectrum was fixed at 0.3 solar; changing the abundance does not change the best fit temperature. The best fit T_x are $kT = 5.8_{-1.7}^{+2.6}$ and

$1.6_{-0.6}^{+0.8}$ keV (one σ uncertainties) for RX J0849+4452 and RX J0848+4453, respectively. These temperatures are in line with the expectations based on the clusters' L_x (Table 1) and the low redshift $L_x - T_x$ relation. This extends to $z \sim 1.3$ the results found up to $z \sim 0.8$ by Donahue et al. (1999) and Della Ceca et al. (2000). The apparent lack of evolution of the $L_x - T_x$ relation to such high redshifts has important implications for both ICM thermodynamics and cosmological models Borgani et al. 2000.

The spectral analysis gives the following results. Within the $r = 35''$ measurement aperture, the observed frame $F_{0.5-6.0} = 1.4_{-0.2}^{+0.2} \times 10^{-14}$ and $0.44_{-0.08}^{+0.08} \times 10^{-14} \text{ ergs cm}^{-2} \text{ s}^{-1}$ for RX J0849+4452 and RX J0848+4453, respectively. The aperture fluxes and luminosities in the rest frame 0.5–2.0 keV band are given in Table 1. The total flux for RX J0849+4452, obtained by extrapolating the best fit King profile, is $F_{0.5-2.0}^{rest} = 1.5_{-0.2}^{+0.2} \times 10^{-14} \text{ ergs cm}^{-2} \text{ s}^{-1}$.

The uncertainties in the quantities presented above were estimated from 10^4 Monte Carlo simulations of the spectra. The simulations are based on the input models for the background and the cluster spectra. The models are folded through the appropriate response matrices and then randomly sampled. The simulated output is fit in the same way as the original spectra. The resulting distribution of temperatures is asymmetric but the median temperature matches the input temperature, showing no strong biases in our method of measuring T_x .

A total mass can be estimated from the T_x , assuming an isothermal sphere and extrapolating the X-ray emission to $r = 1$ Mpc using the best fit profile shown in the right panel of Figure 1. The total mass of RX J0849+4452 derived from the new X-ray data is $4.0_{-1.9}^{+2.4} \times 10^{14} M_\odot$ within $r = 1h_{65}^{-1}$ Mpc. No estimate was calculated for RX J0848+4453 due to its strong departure from spherical symmetry and uncertain T_x . The new L_x for RX J0848+4453 is approximately in line with the expectation according to the present epoch $L_x - \sigma$ relation (e.g. Edge & Stewart 1991; Borgani et al. 1999b) for the estimate we have made of the velocity dispersion $\sigma = 650 \pm 170 \text{ km s}^{-1}$ of its 9 member galaxies for which we have sufficiently high resolution spectra. Member galaxy redshifts have not yet been obtained with sufficient accuracy to enable the calculation of a meaningful velocity dispersion for comparison to the total mass estimate in the case of RX J0849+4452.

4. DISCUSSION

The spatially extended X-ray emission seen in RX J0849+4452 clearly shows that a hot intracluster medium exists in galaxy clusters at $z > 1$. In this cluster the ICM has a regular, centrally concentrated spatial distribution, similar to the relaxed appearance RX J0849+4452 presents in the optical/IR (Figure 3). But the ICM in the other $z > 1$ cluster, RX J0848+4453, is very weak and appears to be divided between the two sides of the cluster. Two groups may be in the process of merging, as appears to be seen also in the distribution of the red galaxies (Figure 3). Using photometric redshifts for all galaxies at $K < 20.6$, nearly 50% of the member galaxies lie within the central 30 arcsec of RX J0849+4452, while only 10% of the probable members are in the same region of RX J0848+4453 (van Dokkum et al., in prepara-

tion). While the two clusters show rather different distributions both in the optical/IR and in the X-ray, they contain galaxy populations dominated by red galaxies which appear to have little or no recent star formation Stanford et al. 1997, Rosati et al. 1999. The median colors of these red galaxies are the same within 0.05 in e.g. $I - K$, and HST imaging of RX J0848+4453 shows them to be overwhelmingly early-types (van Dokkum et al. in preparation). This suggests that the early-type galaxies found in clusters were largely formed prior to cluster formation.

We thank Scott Wolk for assistance with planning our

Chandra observation, and Patrick Wojdowski for help with Chandra data analysis, and the referee for a timely report. Support for SAS came from NASA/LTSA grant NAG5-8430 and for BH from NASA/Chandra GO0-1082A, and both are supported by the Institute of Geophysics and Planetary Physics (operated under the auspices of the US Department of Energy by the University of California Lawrence Livermore National Laboratory under contract W-7405-Eng-48). Portions of this work were carried out by the Jet Propulsion Laboratory, California Institute of Technology, under a contract with NASA.

REFERENCES

- Borgani, S., Rosati, P., Tozzi, P., & Norman, C. 1999, ApJ, 517, 40
 Borgani, S., Girardi, M., Carlberg, R.G., Yee, H.K.C., & Ellingson, E. 1999, ApJ, 527, 561
 Borgani, S., Rosati, P., Tozzi, P., Stanford, S.A., Eisenhardt, P.R., Lidman, C., Holden, B., Norman, C., & Squires, G. 2000, ApJL, submitted
 Bower, R. 1997, MNRAS, 288, 355
 Cash, W. 1979, ApJ, 228, 939
 Crawford, C.S. & Fabian, A. 1996, MNRAS 282, 1483
 Della Ceca, R., Scaramella, R., Gioia, I.M., Rosati, P., Fiore, F., & Squires, G. A&A, 353, 498
 Dickey, J.M. & Lockman, F.J. 1990, ARAA, 28, 215
 Donahue, M., Voit, G.M., Scharf, C.A., Gioia, I.M., Mullis, C.R., Hughes, J.P., & Stocke, J.T. 1999, ApJ, 527, 525
 Edge, A.C. & Stewart, G.C. 1991, MNRAS, 252, 428
 Eke, V., Cole, S., Frenk, C. & Henry, P. 1998, MNRAS, 298, 1145
 Oukbir, J. & Blanchard, A. 1992, A&A, 262, L210
 Raymond, J.C. & Smith, B.W. 1977, ApJS, 35, 419
 Rosati, P., della Ceca, R., Burg, R., Norman, C., & Giacconi, R. 1995, ApJ, 445, L11
 Rosati, P., della Ceca, R., Norman, C., & Giacconi, R. 1998, ApJ, 492, L21
 Rosati, P., Stanford, S. A., Eisenhardt, P., Elston, R., Spinrad, H., Stern, D., & Dey, A. 1999, AJ, 118, 76
 Schlegel, D.J., Finkbeiner, D.P., Davis, M. 1998, ApJ, 500, 525
 Stanford, S. A., Elston, R., Eisenhardt, P., Spinrad, H., Stern, D., & Dey, A. 1997, AJ, 114, 2232
 Tozzi, P. & Norman, C. 2000, ApJ, in press

TABLE 1
 CHANDRA RESULTS^a

Cluster	z	$F[0.5-2.0]^b$ $10^{-15} \text{ erg s}^{-1} \text{ cm}^{-2}$	$L[0.5-2.0]^b$ $10^{44} \text{ erg s}^{-1}$	$L[\text{bol}]^c$ $10^{44} \text{ erg s}^{-1}$	T_x keV	$M_{\text{total}}(< 1 \text{ Mpc})$ $10^{14} M_{\odot}$
RXJ0848+4453	1.27	$1.4^{+0.3}_{-0.3}$	$0.40^{+0.16}_{-0.11}$	$0.69^{+0.27}_{-0.17}$	$1.6^{+0.8}_{-0.6}$...
RXJ0849+4452	1.26	$9.0^{+0.9}_{-0.9}$	$0.51^{+0.05}_{-0.05}$	$3.3^{+0.9}_{-0.5}$	$5.8^{+2.8}_{-1.7}$	$4.0^{+2.4}_{-1.9}$

^a $H_0 = 65 \text{ km s}^{-1} \text{ Mpc}^{-1}$, $\Omega_m = 0.3$, and $\Lambda = 0.7$ are assumed.

^b $r = 35''$ aperture

^caperture corrected to total

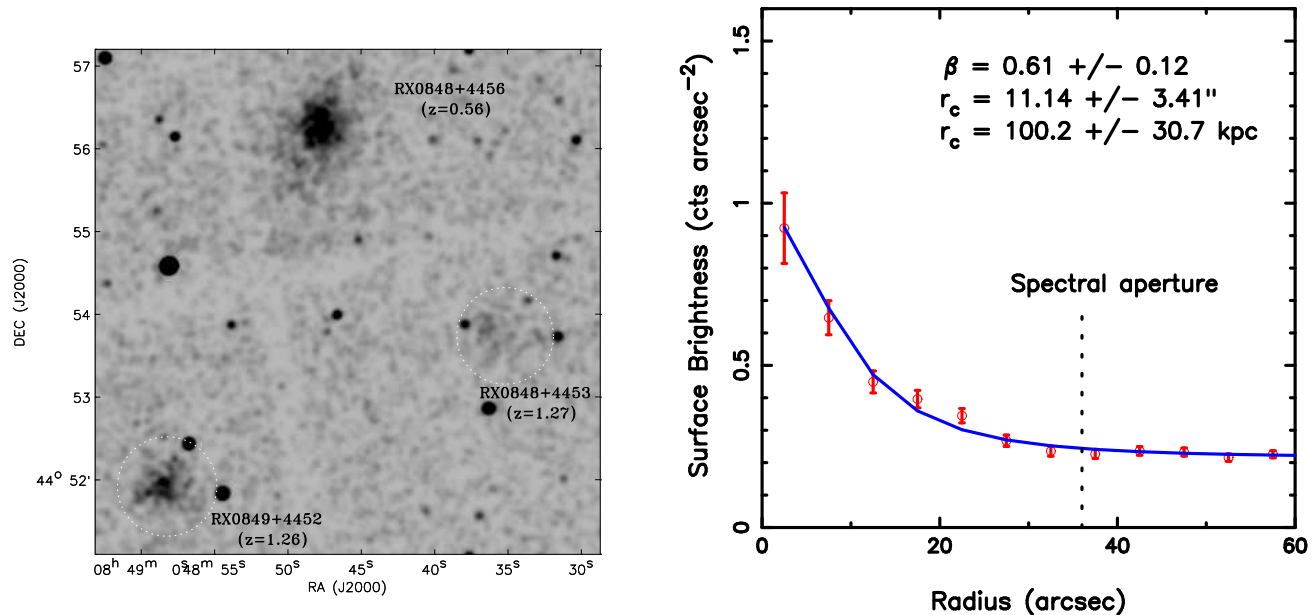


FIG. 1.— (left) Greyscale image of the ACIS-I data showing a 6×6 arcmin field. The image has been smoothed by a two-dimensional Gaussian with $\sigma = 2.1$ arcsec. The apertures used for making spectra are shown by dashed circles around the two higher- z clusters; the point sources in these apertures were excluded when creating the spectra. (right) Radial profile of the X-ray emission centered on RX J0849+4452 shown by the small circles with one σ errorbars. A β model fit is shown by the line, and the best fit parameters are indicated.

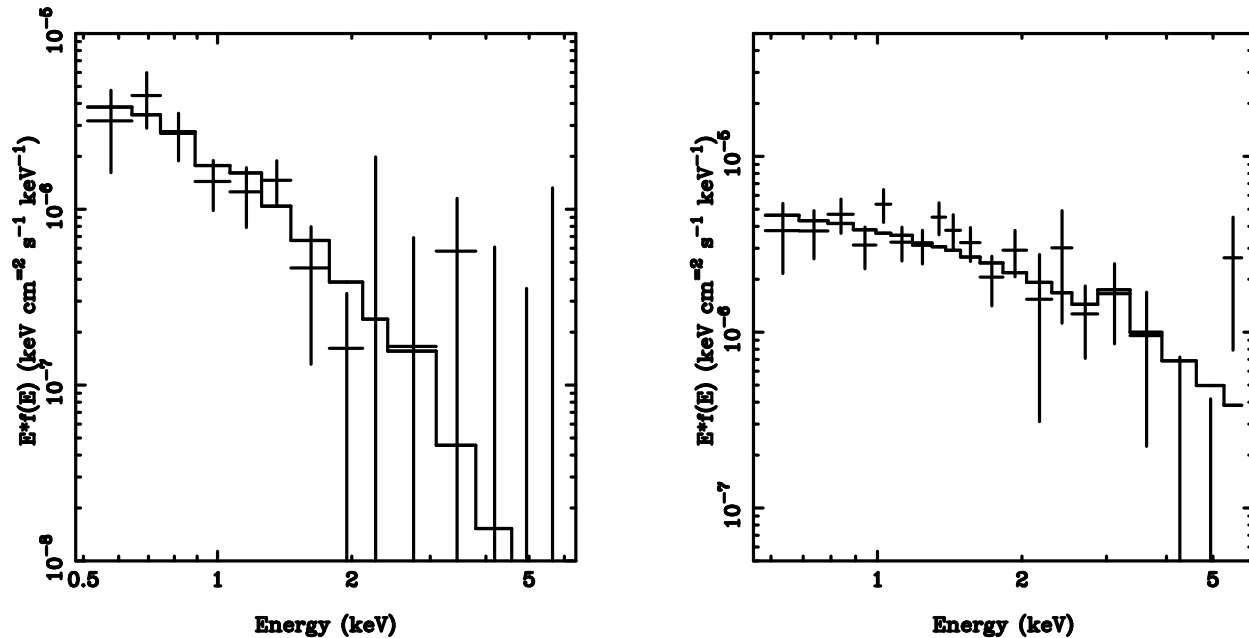


FIG. 2.— ACIS-I unfolded spectra of RX 0848+4453 at $z = 1.27$ (left) and RX J0849+4452 (right; $z = 1.26$) with the fitted models.

FIG. 3.— *BIK* images Stanford et al. 1997, Rosati et al. 1999 showing a 2×2 arcmin field on RX J0848+4453 (left; $z = 1.27$) and RX J0849+4452 (right; $z = 1.26$) with contour overlays (at the levels of $2.5, 5, 7, 15\sigma$) of the X-ray emission detected by Chandra/ACIS-I. The strong X-ray point sources centered on optical objects in the vicinity of the cluster cores are unlikely to be associated with the clusters. In RX J0848+4453 (left), the relatively bright source at lower left, which is associated with a red galaxy, is a known quasar at $z = 1.194$. In RX J0849+4452 (right), the relatively bright X-ray source to the north of the cluster core is associated with a quasar at $z = 1.329$.

This figure "stanford_fig3a.jpg" is available in "jpg" format from:

<http://arxiv.org/ps/astro-ph/0012250v1>

This figure "stanford_fig3b.jpg" is available in "jpg" format from:

<http://arxiv.org/ps/astro-ph/0012250v1>